

UCLA

UCLA Previously Published Works

Title

Thin film interference in the optomechanical response of micromechanical silicon cantilevers

Permalink

<https://escholarship.org/uc/item/7fp7k2ct>

Journal

Applied Physics Letters, 89(24)

ISSN

0003-6951

Authors

Wilkinson, P R
Gimzewski, J K

Publication Date

2006-12-01

Peer reviewed

Thin film interference in the optomechanical response of micromechanical silicon cantilevers

Paul R. Wilkinson

Department of Chemistry and Biochemistry, University of California, Los Angeles, California 90095

James K. Gimzewski^{a)}

Department of Chemistry and Biochemistry, University of California, Los Angeles, California 90095 and California Nanosystems Institute, Los Angeles, California 90095

(Received 27 September 2006; accepted 9 November 2006; published online 13 December 2006)

The mechanical response of uncoated silicon microcantilevers is shown to modulate as a function of incident wavelength. Cantilever motion is measured interferometrically, using phase sensitive detection in response to a mechanically chopped excitation source. Thin film interference modeling shows that the fraction of absorbed light within the cantilever varies periodically over the range of 450–1000 nm, in excellent agreement with the measurements. The results show that the optomechanical responsivity of these cantilevers can be tuned due to the effect via an appropriate selection of incident wavelength, incidence angle, lever thickness, and optical constants of the lever. © 2006 American Institute of Physics. [DOI: 10.1063/1.2405887]

The optomechanical response (OMR) of micromechanical cantilevers, a mechanical deflection due to an optical stimulus, was first noted early in the development of atomic force microscopy (AFM), where this phenomenon was used to drive a Ni foil cantilever at its resonance frequency for a dynamic mode AFM.¹ Several important mechanisms involved in the OMR have been investigated for both silicon nitride² and silicon cantilevers.³ The OMR has been used primarily as a single wavelength technique to drive a cantilever at or near its resonance frequency for dynamic mode AFM (Refs. 1 and 4) and as a driving mechanism for nanoelectromechanical oscillators.⁵ Barnes *et al.* employed a broadband optical source and monochromator to obtain cantilever-based photothermal spectra of samples in the picogram regime.⁶

The OMR has been attributed to photon pressure,² thermal strain,^{1–6} and electronic strain due to photoexcitation of electrons.³ In each case, the incident light perturbs the lever from thermal and electronic equilibrium, and the steady state depends strongly on the rate of relaxation of the lever by thermal and electronic means.

AFMs typically use silicon or silicon nitride cantilevers, usually with a metallic coating to increase reflectivity, so that shot noise is reduced in optical detection schemes. Here we demonstrate a strategy to increase the reflectivity of the lever while simultaneously decreasing the OMR. The use of thin film interference, which is a highly tunable and predictable, suggests an alternative to metallic coatings.

Uncoated, monocrystalline silicon cantilevers of length, width, and thickness of 500, 100, and 0.9 μm , respectively, were used in this experiment. Cantilever arrays were manufactured at IBM via a proprietary dry etch, silicon on insulator process so that the $\langle 110 \rangle$ direction lies along the cantilever length, with the top face normal to the $\langle 100 \rangle$ direction. In the experimental setup (Fig. 1), cantilever motion was detected interferometrically using a homodyne external Fabry-Pérot interferometer based on a design by Rugar *et al.*⁷ The wavelength of the probe laser was 1311 nm, a photon

energy which is well below the indirect band gap of silicon (at 1050 nm). Light from a 100 W xenon lamp was mechanically chopped at 100 Hz, focused into a monochromator coupled to an optical fiber and directed at the cantilever. The signal from the interferometer was analyzed using a phase sensitive detection scheme as a function of excitation wavelength. The resulting spectra were normalized by the excitation spectrum of the lamp [Fig. 2(a)].

The cantilever is modeled as an absorbing thin film,⁸ upon which monochromatic plane waves are incident from a nonabsorbing medium of refractive index, $n_1=n_3=1$. Mathematically, the film is characterized by a thickness h and a complex index of refraction $\hat{n}_2=n_2-ik_2$. From the Fresnel equations, we find the reflection and transmission coefficients, r and t , respectively, which we write as complex quantities,

$$r_{jk} = \rho_{jk} e^{i\phi_{jk}},$$

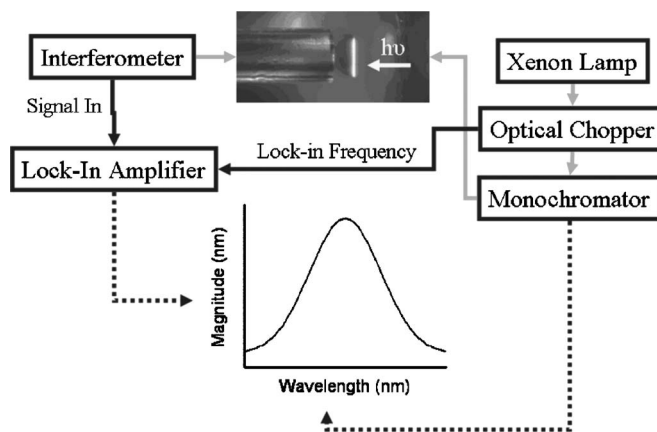


FIG. 1. Schematic of the experimental setup for obtaining an OMR spectrum. In the photograph, the cantilever is extending toward the viewer, out of the plane of the page. The detection fiber from the interferometer is shown to the left, but the excitation fiber is not visible. The white arrow, together with the text $h\nu$, represents the excitation source emerging from the excitation fiber to the right of the cantilever.

^{a)}Electronic mail: gim@chem.ucla.edu

$$t_{jk} = \tau_{jk} e^{i\chi_{jk}}. \tag{1}$$

The sums of all of the plane waves which are reflected r_{tot} or transmitted t_{tot} from the film are found using the formulas derived by Airy,⁹ and a third equation for the amplitude of the standing waves s_{tot} within the film is derived in an analogous manner,

$$r_{\text{tot}} = \frac{r_{12} + r_{23} e^{-i2\beta h}}{1 + r_{12} r_{23} e^{-i2\beta h}},$$

$$t_{\text{tot}} = \frac{t_{12} t_{23} e^{-i\beta h}}{1 + r_{12} r_{23} e^{-i2\beta h}},$$

$$s_{\text{tot}} = \frac{t_{12} e^{-i\beta z} + t_{12} r_{23} e^{-i\beta(2h-z)}}{1 + r_{12} r_{23} e^{-i2\beta h}}, \tag{2}$$

where

$$\beta \equiv \frac{2\pi}{\lambda_0} \hat{n}_2 \cos(\hat{\theta}_2). \tag{3}$$

Here λ_0 is the wavelength of the incident light in a vacuum and θ_2 is the complex angle of refraction. The reflectivity, transmissivity, and standing waves are found from the squared modulus of Eqs. (2),

$$R = \frac{\rho_{12}^2 + \rho_{23}^2 e^{-\Im(4\beta h)} + 2\rho_{12}\rho_{23} e^{-\Im(2\beta h)} \cos(\Re(2\beta h) + \phi_{23} - \phi_{12})}{1 + \rho_{12}^2 \rho_{23}^2 e^{-\Im(4\beta h)} + 2\rho_{12}\rho_{23} e^{-\Im(2\beta h)} \cos(\Re(2\beta h) + \phi_{23} + \phi_{12})},$$

$$T = \frac{n_3 \cos(\theta_3)}{n_1 \cos(\theta_1)} \frac{\tau_{12}^2 \tau_{23}^2}{1 + \rho_{12}^2 \rho_{23}^2 e^{-\Im(4\beta h)} + 2\rho_{12}\rho_{23} e^{-\Im(2\beta h)} \cos(\Re(2\beta h) + \phi_{23} + \phi_{12})},$$

$$A = 1 - R - T,$$

$$S = \frac{\tau_{12}^2 e^{-\Im(2\beta z)} + \tau_{12}^2 \rho_{23}^2 e^{-\Im(2\beta(2h-z))} + 2\tau_{12}^2 \rho_{23} e^{-\Im(2\beta(h-z))} \cos(\Re(2\beta(h-z)) + \phi_{23})}{1 + \rho_{12}^2 \rho_{23}^2 e^{-\Im(4\beta h)} + 2\rho_{12}\rho_{23} e^{-\Im(2\beta h)} \cos(\Re(2\beta h) + \phi_{23} + \phi_{12})}. \tag{4}$$

The parameters used in this model were an incidence angle of 0° , the refractive index of the surrounding medium is assumed to be 1 for all wavelengths, and $h=0.9 \mu\text{m}$. Literature values for the optical constants of pure silicon were used for the wavelengths of interest.¹⁰ The results of the model for R , T , and A are presented in Fig. 3, and the standing waves S are presented in Fig. 2(b).

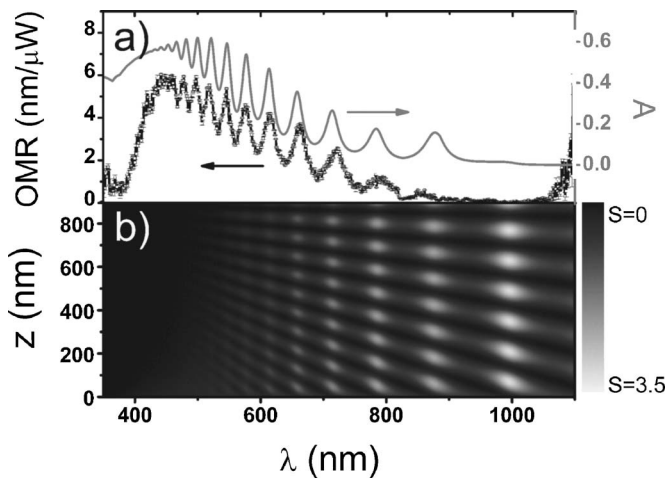


FIG. 2. (a) Excitation wavelength dependence of the OMR showing thin film interference in an uncoated silicon cantilever as determined experimentally, as well as the absorbance A determined from Eq. (4). (b) Standing waves across the thickness coordinate of the cantilever z presented as a function of excitation wavelength, as determined by Eq. (4). Bright regions in Fig. 3(b) correspond to optically bright spots within the cantilever, and dark areas are regions where the light is of low intensity within the cantilever.

We find excellent agreement between experiment and theory both in the positions and magnitudes of the interference peaks. Light from the excitation source enters the cantilever from the top side and reflects internally multiple times across the thickness of the lever, resulting in interference. Light of appropriate wavelengths can form standing waves across the lever [Fig. 2(b)] as a result of constructive interference. This leads to increased absorption; since a linear relationship has been demonstrated between absorbed power and cantilever deflection,^{1,5,11,12} an increased OMR is ob-

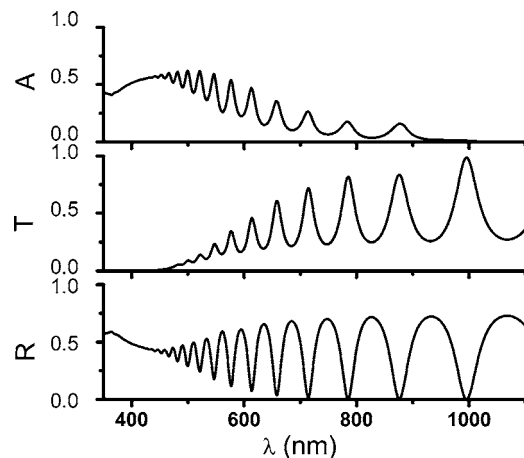


FIG. 3. Results from Eq. (4), the wavelength dependence of the thin film model, showing the reflected (R), transmitted (T), and absorbed (A) fractions of incident light for parameters corresponding to the experimental geometry [$\theta_1=0$, $n_1(\lambda)=n_3(\lambda)=1$, $h=900 \text{ nm}$, and $\hat{n}_2(\lambda)$ from literature values].

served. Similarly, a destructive interference of waves within the lever results in a decreased OMR.

At long wavelengths ($\lambda > 900$ nm), κ is small, so absorption is minimal and the standing waves are intense. At short wavelengths ($\lambda < 450$ nm), κ is large, so any wave traveling across the thickness of the lever is attenuated significantly before it is reflected and no interference is observed in this region. In the intermediate range ($450\text{nm} < \lambda < 900$ nm), the wave is attenuated enough that an OMR is observed yet there is still sufficient amplitude on reflection to result in an observed interference signal.

Previously, the OMR was modeled and maximized with respect to the thermal signal by a mechanical approach,¹² namely, by optimizing the thickness ratio of cantilever materials with highly differing thermal expansion coefficients, resulting in a 40% increase in the OMR. The mechanical amplification of the thermal signal results in an increase in the OMR at all wavelengths, whereas thin film interference can be used to fine tune the OMR at a particular wavelength and can be used in conjunction with the mechanical strategy.

From the data in Fig. 2(a), the OMR is increased by $\sim 50\%$ at 660 nm and decreased by $\sim 50\%$ at 635 nm due to the optical strategy. These are two common wavelengths for commercial laser diodes, but the use of either one with the cantilever will give different results. From Fig. 3, this cantilever is highly reflective to 660 nm light, with a small OMR due to destructive interference within the lever. Conversely, the lever has a low reflection coefficient at 635 nm and exhibits twice the OMR at this wavelength than at 660 nm. A 660 nm laser is an appropriate choice for detecting the cantilever motion without perturbing it, whereas a 635 nm laser is an appropriate choice where one desires to oscillate the cantilever optically.

One consequence of the OMR is the effect of optomechanical noise in Scanning Probe Microscopy or cantilever-based experiments. In its simplest form the OMR can be written as a linear relationship $z = C_{\text{OM},\lambda} I_0$, where z is the displacement of the tip in nanometers, $C_{\text{OM},\lambda}$ is defined as an optomechanical coefficient at a particular wavelength of light, and I_0 is the intensity of the incident light. The use of intensity in this expression implies that the light is uniform across the whole lever. The optomechanical noise is then $\langle dz \rangle = C_{\text{OM},\lambda} \langle dI_0 \rangle$. This simple expression implies that care should be taken in experimental parameters such as the

wavelength of the probe laser that is used to detect the cantilever motion.

Thin film interference has been employed as a simultaneous reflectance increasing and noise reducing strategy in ultrasensitive force detection^{13,14} at millikelvin temperatures where thermal fluctuations dominate the noise floor. The advantage of a thin film interference scheme is twofold. An interference maximum in the reflectance spectrum of an uncoated lever is coincidentally an absorption minimum (see Fig. 3). Shot noise is decreased by increasing the reflectivity of the lever, while the optomechanical noise is simultaneously decreased via destructive interference within the lever. Metallic coatings have been traditionally used to increase the reflectivity but have been shown to be an effective way to increase the thermal component of $C_{\text{OM},\lambda}$.^{11,12}

We report the wavelength dependence of the OMR of uncoated silicon micromechanical cantilevers. The modulation of the OMR as a function of wavelength is shown to be consistent in magnitude and position with thin film interference. The data suggest an optical strategy for tuning OMR as well as the reflectivity of the cantilever at a particular wavelength.

¹N. Umeda, S. Ishizaki, and H. Uwai, *J. Vac. Sci. Technol. B* **9**, 1318 (1991).

²O. Marti, A. Ruf, M. Hipp, H. Bielefeldt, J. Colchero, and J. Mlynek, *Ultramicroscopy* **42-44**, 345 (1992).

³Albert Prak and Theo S. J. Lammerink, *J. Appl. Phys.* **71**, 5242 (1992).

⁴Glenn C. Ratcliff, Dorothy A. Erie, and Richard Superfine, *Appl. Phys. Lett.* **72**, 1911 (1998).

⁵B. Ilic, S. Krylov, K. Aubin, R. Reichenbach, and H. G. Craighead, *Appl. Phys. Lett.* **86**, 193114 (2005).

⁶J. R. Barnes, R. J. Stephenson, M. E. Welland, Ch. Gerber, and J. K. Gimzewski, *Nature (London)* **372**, 79 (1994).

⁷D. Rugar, H. J. Mamin, and P. Guethner, *Appl. Phys. Lett.* **55**, 25 (1989).

⁸M. Born and E. Wolf, *Principles of Optics*, 7th ed. (Cambridge University Press, New York, 1999), pp. 752-759.

⁹G. B. Airy, *Philos. Mag.* **2**, 12 (1833).

¹⁰*CRC Handbook of Chemistry and Physics*, 87th ed. (CRC, Boca Raton, FL, 2006).

¹¹J. Varesi, J. Lai, T. Perazzo, Z. Shi, and A. Majumdar, *Appl. Phys. Lett.* **71**, 306 (1997).

¹²J. Lai, T. Perazzo, Z. Shi, and A. Majumdar, *Sens. Actuators, A* **58**, 115 (1997).

¹³D. Rugar, B. C. Stipe, H. J. Mamin, C. S. Yannoni, T. D. Stowe, K. Y. Yasumura, and T. W. Kenny, *Appl. Phys. A: Mater. Sci. Process.* **72**, S3 (2001).

¹⁴H. J. Mamin and D. Rugar, *Appl. Phys. Lett.* **79**, 3358 (2001).